*Int. J. Multiphase Flow* Vol. 14, No. 5, pp. 645–652, 1988
Printed in Great Britain. 

0301-9322/88 $3.00 + 0.00


# BRIEF COMMUNICATION

# VOID DISTRIBUTIONS IN BUBBLY FLOW THROUGH YAWED ROD ARRAYS

J. T. ROBINSON,† N. E. TODREAS and D. EBELING-KONING‡
Department of Nuclear Engineering, Massachusetts Institute of Technology, Cambridge, MA 02139, U.S.A.

(*Received* 2 *December* 1986; *in revised form* 17 *May* 1988)

## 1. INTRODUCTION

In this communication observations of void distribution in bubbly flow through an array of rods inclined relative to the average flow direction are presented. The experiments reveal a strong dependence of void distribution on bubble size and rod arrangement. It is postulated that this dependence is due to the entrapment and migration of bubbles in vortices behind the rods. Not surprisingly, attempts to simulate the experimental results with a six-equation porous body model, in which localized phenomenon such as vortices have been averaged out, were unsuccessful.

## 2. EXPERIMENTS

Figure 1 is a sketch of the flow field considered in this study, an air–water bubbly mixture flowing vertically upward through an inclined rod array. The inclination angle of the rods relative to the vertical was 45°. The flow through arrays of two rod arrangements, inline square and rotated square was considered. Rod arrangements are defined according to the average direction of the transverse (normal to the rod axis) component of flow relative to the layout of the rod array, as illustrated in figure 2. Characteristics of each rod array and the experimental conditions are listed in table 1. The superficial velocities $j_L$ and $j_G$ are defined by

$$j_k = \frac{\dot{m}_k}{\gamma_v A_{xs}}, \qquad [1]$$

where $k$ represents phase ($L$ for liquid, G for gas), $\dot{m}_k$ is the mass flow rate of phase $k$, $A_{xs}$ is the total cross-sectional area of the bundle and $\gamma_v$ is the bundle porosity, defined as the ratio of fluid volume to total volume.

### *2.1. Inline square array*

Void distributions in the inline 45° test section were observed for a range of gas and liquid flow rates ($0 < j_G < 0.3$ m/s, $0 < j_L < 1$ m/s). Details of the study are given in Ebeling-Koning (1983). Figures 3 and 4 show the flow development through the test section for two liquid flow rates. Figures 5 and 6 are photographs of the exit plenum for a range of gas and liquid flow rates. The most striking observation from these plates is the influence of bubble size on void distribution. At low liquid flow rates a wide distribution of bubble sizes is generated. The large bubbles drift to the right wall across the rods, as predicted by the porous body model. However, the smaller bubbles migrate along the rod axis to the left wall. At high liquid flow rates only small bubbles exist. These also move along the rod axis until they meet the left wall.

†‡Present addresses: †Engineering Physics and Mathematics Division, Oak Ridge National Laboratory, Oak Ridge, TN 37831; and ‡Nuclear Technology Systems Division, Westinghouse Electric Corporation, P.O. Box 355, Pittsburgh, PA 15230, U.S.A.

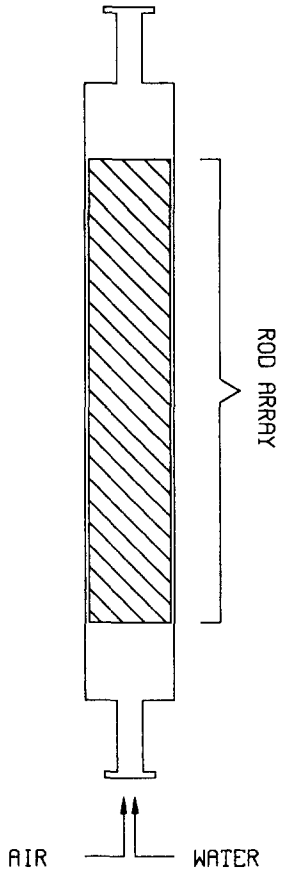


Figure 1. Experimental arrangement.

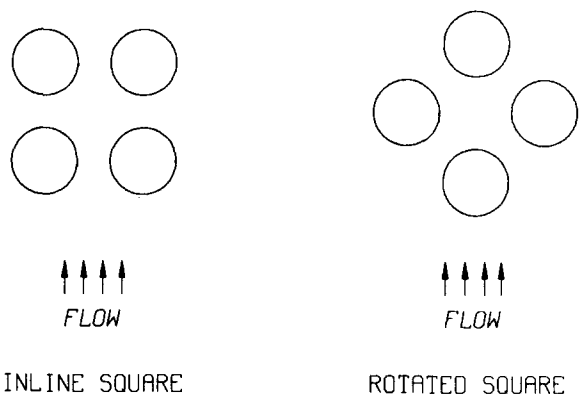


Figure 2. Rod arrangements.

### 2.2. *Rotated square array*

The phenomenon of bubble migration along the rod axis was not observed in the rotated square inclined rod array. The void distributions appeared to be either flat or skewed slightly to the right (across the rods) over the entire range of flow rates observed ($0 < j_G < 0.3$ m/s, $0 < j_L < 1$ m/s).

## 3. DISCUSSION

To understand the observed motion of small bubbles in the inline array as well as the rod arrangement effect, it is helpful to consider the characteristics of flow around submerged cylinders. This flow can be divided into three regions: a mainstream region; a boundary layer blanketing the solid surface; and a region of recirculating flow between the separated boundary layer and the trailing edge of the solid surface. For flow across a cylinder the boundary layer separates in the

Table 1. Test section dimensions

| | Inclined (45°) rod arrays | | Transverse rod arrays | |
|---|---|---|---|---|
| | Inline square | Rotated square | Inline square | Rotated square |
| Pitch/diameter ratio | 1.5 | 1.5 | 1.5 | 1.5 |
| Rod diameter (m) | 0.0064 | 0.0127 | 0.0127 | 0.0127 |
| Length (cm) | 91 | 71 | 28 | 28 |
| Width (cm) | 17 | 15 | 5.7 | 15 |
| Depth (cm) | 7.3 | 5.4 | 5.1 | 5.4 |

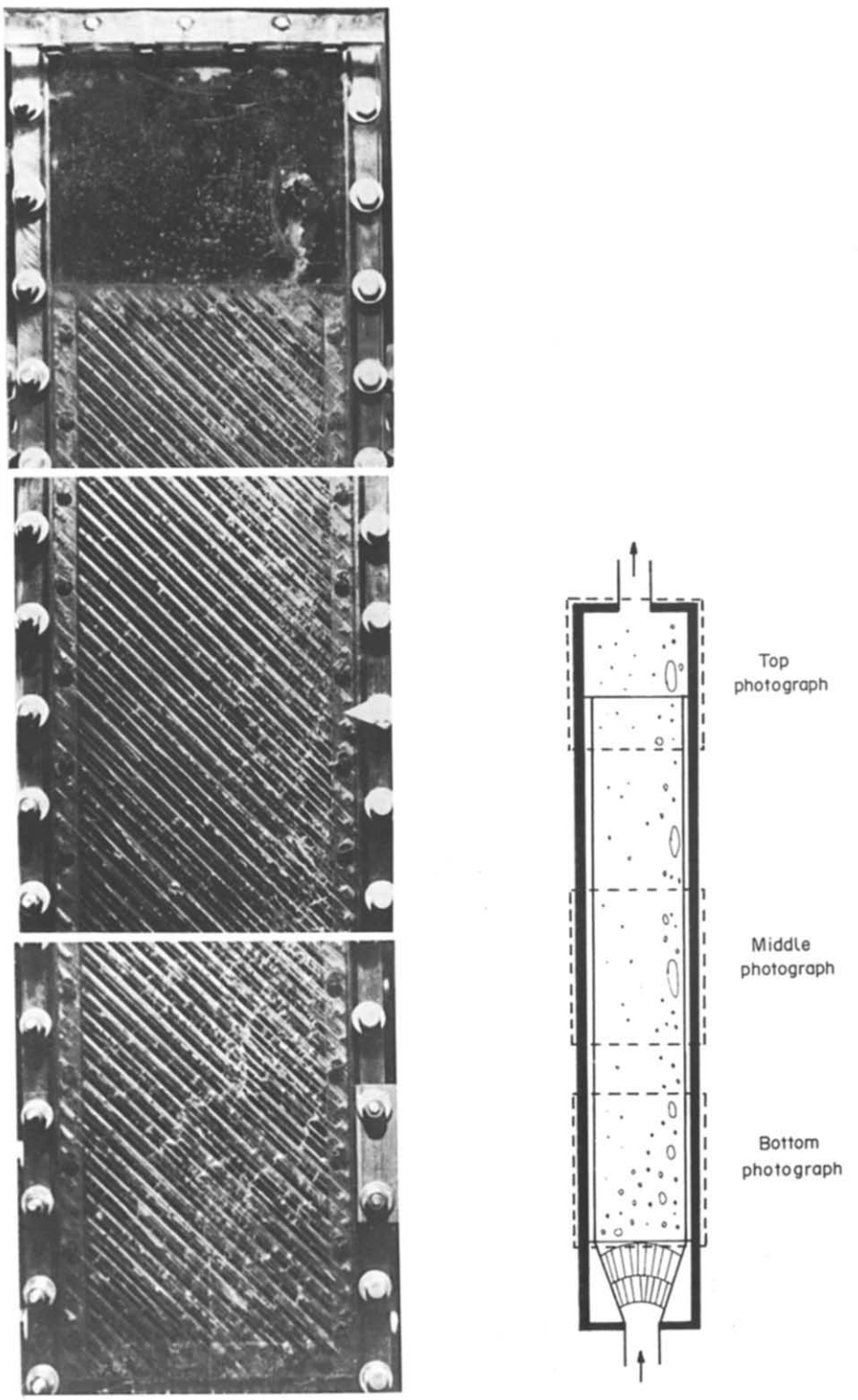


Figure 3. Flow pattern in inline square inclined flow test section for low liquid flow rate. $j_L = 0.15$ m/s, $j_G = 0.08$ m/s.

vicinity of 80°–90° from the leading edge, resulting in two vortices behind the cylinder (Hoerner 1965). In an array of rods a similar flow pattern exists. However, the size of the vortices is dependent on the rod arrangement. Photographs by Hoerner (1965), as well as Wallis (1939), show that the vortices in inline square rod arrays approximately fill the area between rods of adjacent

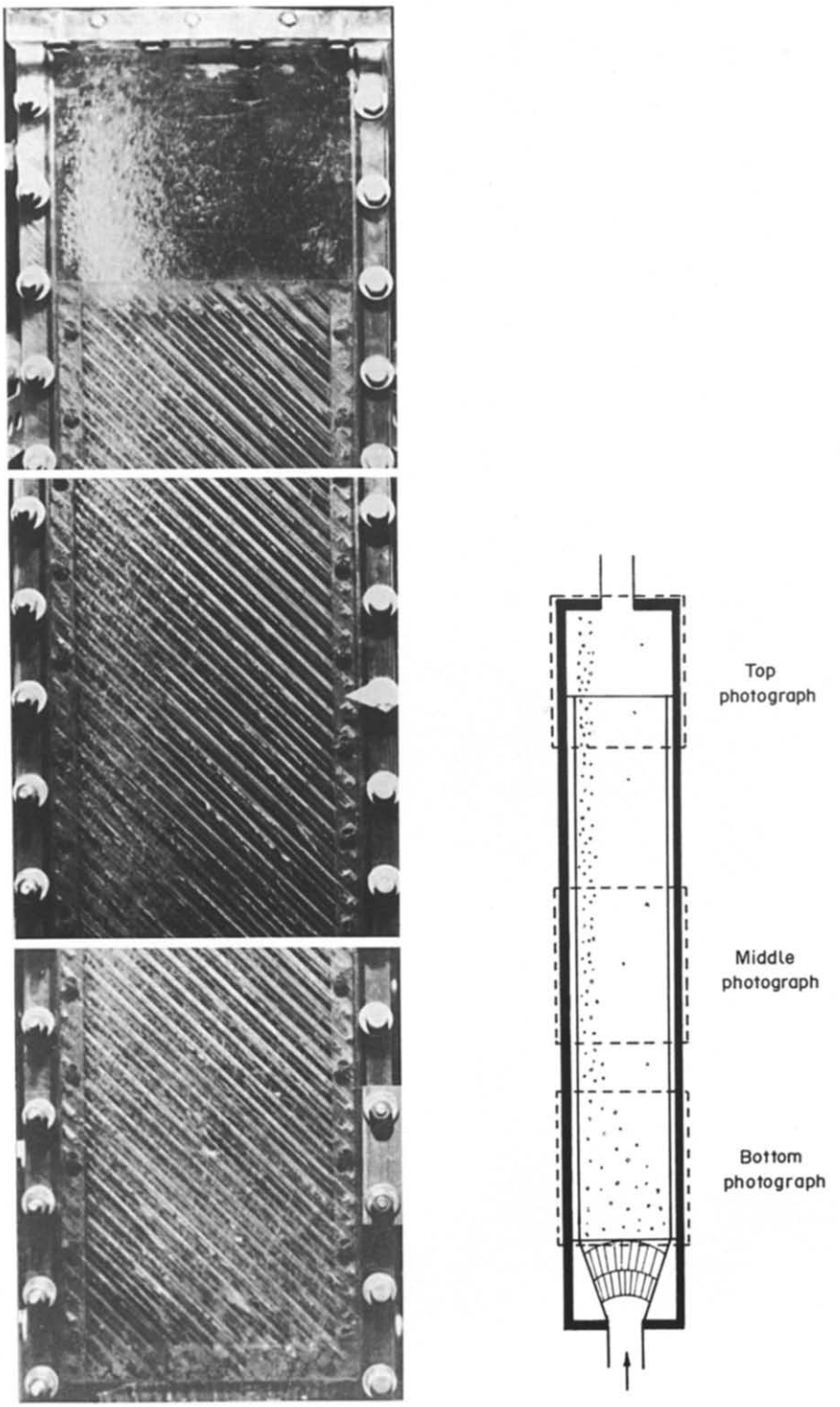


Figure 4. Flow pattern in inline square inclined flow test section for high liquid flow rate. $j_L = 0.86$ m/s, $j_G = 0.08$ m/s.

rows. We confirmed this finding in an inline square transverse (90° to flow) rod array. (Vortices were observed with the aid of the dispersed air bubbles.) However, in a rotated square transverse rod array of comparable dimensions the vortices were found to be very small. This observation is consistent with the work of Simonin *et al.* (1987) who made measurements of the velocity field

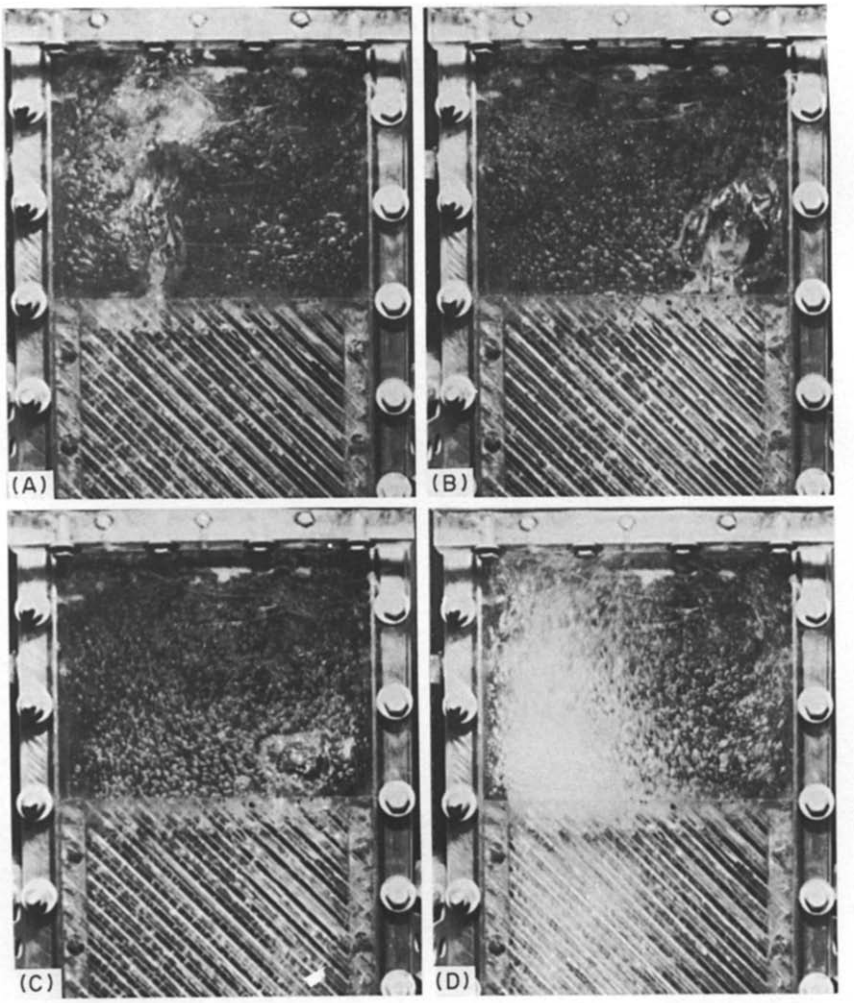


Figure 5. Flow distribution at exit plenum of inline square inclined flow test section for $j_G = 0.27$ m/s. (A) $j_L = 0.00$ m/s; (B) $j_L = 0.15$ m/s; (C) $j_L = 0.35$ m/s; (D) $j_L = 0.86$ m/s.

in a rotated square bundle using laser doppler anemometry. Characteristics of our transverse rod arrays are given in table 1.

Based on these observations, a hypothesis was formulated to explain the small bubble motion in the inline array. Namely, small bubbles have a tendency to migrate into the recirculating zone where they become entrapped. The swirling vortex acts as a centrifuge forcing the lighter bubbles towards its center. The entrapped bubbles then are transported parallel to the rod by pressure and/or drag forces. This hypothesis explains the lack of observed bubble migration along the rod axis in the rotated square rod array since the vortices in this array are small. Observed trajectories of individual bubbles from time-exposed photographs also seem to support this hypothesis. Figure 7 is a time-lapse photograph of a small bubble in the inline rod array. It appears that the bubble follows a helical path confined between the rods, which would be expected of a bubble entrapped in a vortex.

## 4. POROUS BODY MODEL PREDICTIONS

These results have significance regarding the interpretation of predictions of the two-fluid porous body model (Ishii 1975), which is a widely used tool for multidimensional two-phase flow studies in the nuclear industry. The basic equations of this model are time- and volume-averaged forms

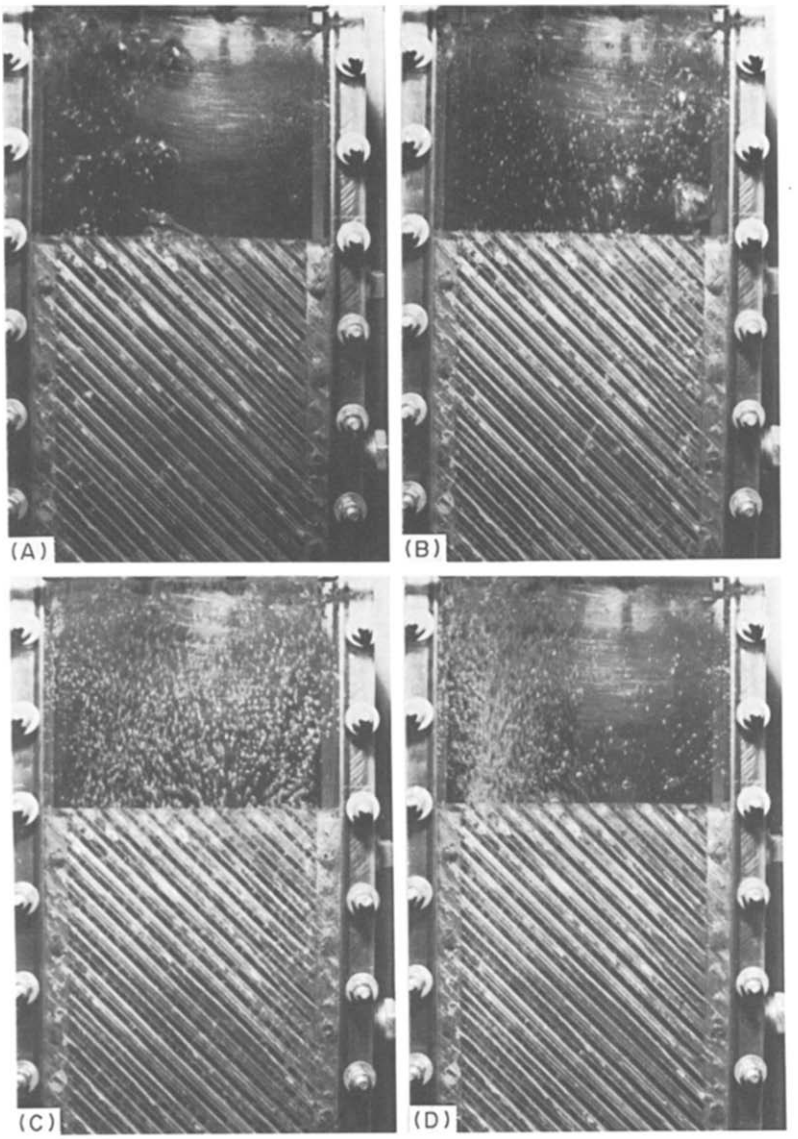


Figure 6. Flow distribution at exit plenum of inline square inclined flow test section for $j_G = 0.014$ m/s. (A) $j_L = 0.00$ m/s; (B) $j_L = 0.15$ m/s; (C) $j_L = 0.35$ m/s; (D) $j_L = 0.60$ m/s.

of the conservation laws (mass, momentum and energy). The model requires as input, constitutive relations for the interfacial shear between the phases and the fluid–solid flow resistance. These relations have in the past been derived from experiments in simple one-dimensional geometries, specifically stagnant pools, parallel rod arrays and crossflow rod arrays. It has been either explicitly or implicitly assumed that these constitutive relations can be applied to multidimensional flows, either by applying an isotropic assumption or various superposition schemes.

An implementation of the porous body model, as derived by Ebeling-Koning (1983), was used to calculate void fraction distributions in the inline square rod array. Representative results are shown in figure 8. These calculations differ markedly from our experimental observations in that no bubble motion along the rod axes (right to left) is predicted. This is due to the fact that within the context of the porous body model the motion of bubbles is governed by the volume-averaged pressure and velocity fields. For flow through an inclined rod array the average pressure gradient, and hence predicted bubble drift, is generally oriented towards the crossflow direction due to a larger resistance to flow in that direction.

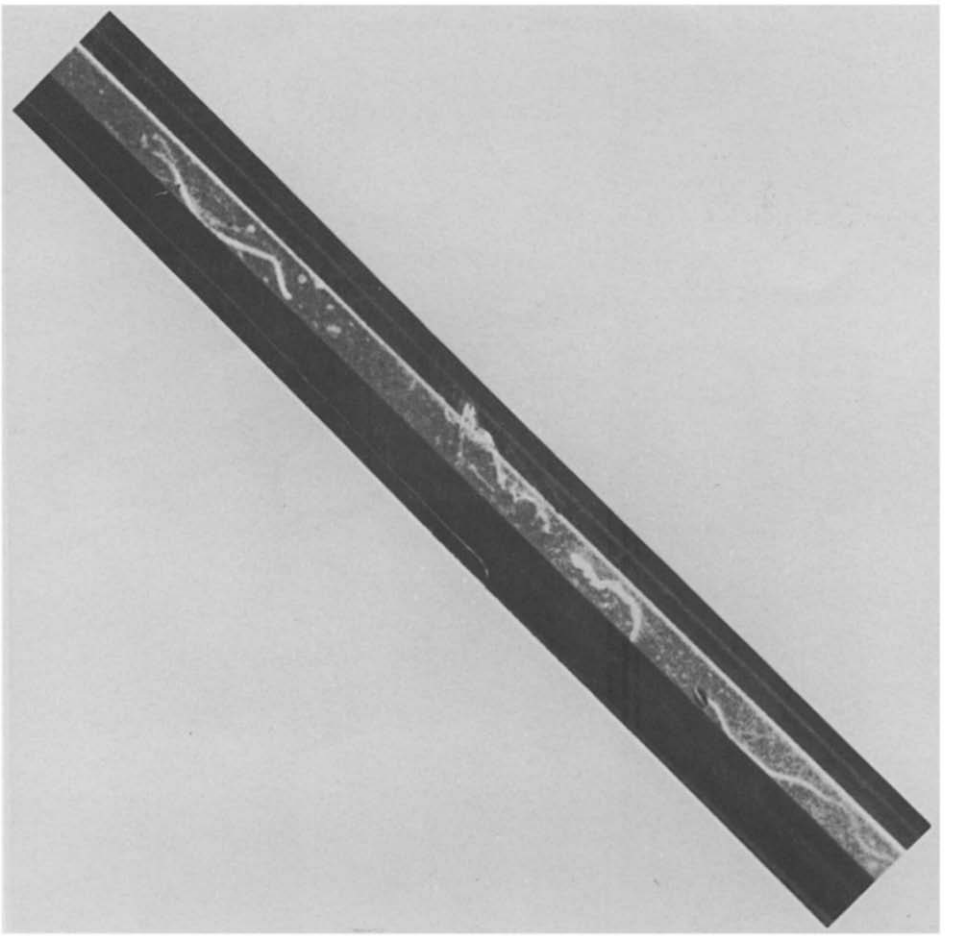

Figure 7. Bubble trajectories in the recirculating region of the inline square inclined flow test section.

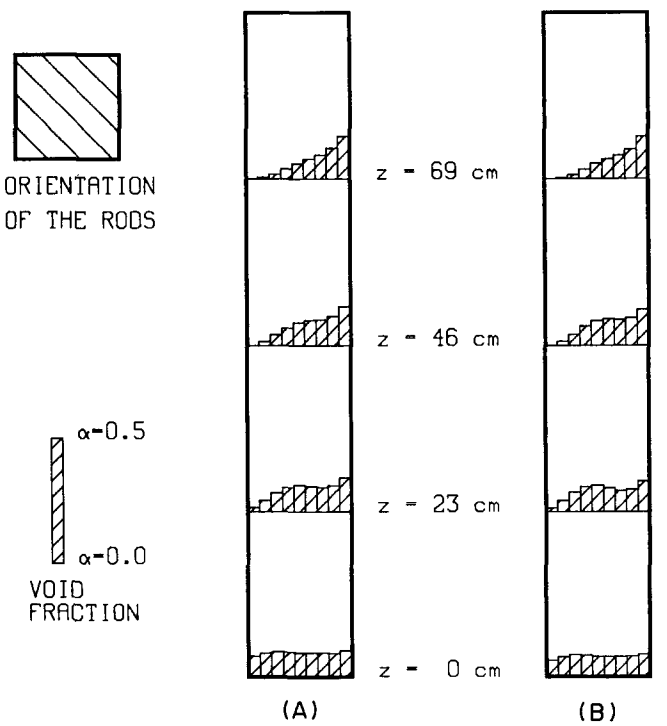


Figure 8. Void distributions computed with the porous body model. (A) $j_L = 0.86$ m/s, $j_G = 0.09$ m/s; (B) $j_L = 1.6$ m/s, $j_G = 0.16$ m/s.

*Acknowledgements*—This work was conducted with the financial support of the U.S. Department of Energy, Office of Basic Energy Sciences.

The authors are grateful to Mssrs P. L. Viollet and O. Simonin of the Laboratoire National d'Hydraulique, Electricité de France (EdF), for much valuable input. The use of EdF computing facilities is also gratefully acknowledged.

## REFERENCES

EBELING-KONING, D. 1983 Hydrodynamics of single- and two-phase flow in inclined rod arrays. Ph.D. Thesis, Dept of Nuclear Engineering, MIT, Cambridge, Mass.

HOERNER, S. F. 1965 *Fluid-dynamic Drag*. Hoerner Fluid Dynamics, 2 King Lane, Bricktown, N.J.

ISHII, M. 1975 *Thermo-fluid Dynamic Theory of Two-phase Flow*. Eyrolles, Paris.

SIMONIN, O., ROBINSON, J. T. & BARCOUDA, M. 1987 Measurements and computations of turbulent flows across a staggered tube bundle. In *Topics in Industrial Hydraulics: Proc. Tech. Session C2 XXII Congr. Int. Ass. Hydraul. Res.*, Ecole Polytechnique Federale, Lausanne, Switzerland.

WALLIS, R. P. 1939 Photographic study of fluid flow between banks of tubes. *Engineering* **148,** 423–426.